ISSN 1063-7842, Technical Physics, 2010, Vol. 55, No. 3, pp. 395–399. © Pleiades Publishing, Ltd., 2010.
Original Russian Text © V.M. Mukhortov, Yu.I. Golovko, A.A. Mamatov, O.M. Zhigalina, A.N. Kuskova, A.L. Chuvilin, 2010, published in Zhurnal Tekhnicheskoĭ Fiziki, 2010, Vol. 80, No. 3, pp. 77–82.

SOLID STATE ELECTRONICS

Effect of Internal Strain Fields on the Controllability of Nanodimensional Ferroelectric Films in a Plane Capacitor

V. M. Mukhortov[a], Yu. I. Golovko[a], A. A. Mamatov[a], O. M. Zhigalina[b], A. N. Kuskova[b], and A. L. Chuvilin[c]

[a] *South Scientific Center, Russian Academy of Sciences, ul. Chekhova 41, Rostov-on-Don, 344006 Russia*
e-mail: muhortov@rambler.ru
[b] *Shubnikov Institute of Crystallography, Russian Academy of Sciences, Leninskii pr. 59, Moscow, 119333 Russia*
[c] *University of Ulm, Ulm, 89069 Germany*

Received July 8, 2009

Abstract—Nanodimensional ferroelectric heteroepitaxial $Ba_{0.8}Sr_{0.2}TiO_3$ films grown by the layer-by-layer mechanism on MgO(100) substrates are examined by the X-ray diffraction and transmission electron microscopy methods. It is established that, when the thickness of the film changes, the stress relaxation proceeds via generation of misfit dislocations at the film–substrate interface. There exists a critical thickness (≈40 nm) of the film below and above which the film possesses tensile and compression stresses, respectively. Examples of how the stresses influence the insulating properties of the films are given.

DOI: 10.1134/S1063784210030102

INTRODUCTION

Barium strontium titanate heterostructures (Ba, Sr)TiO_3 (BST) grown on MgO(100) substrates are being extensively investigated with the aim to use them as new-generation electronically controlled elements in ultra-high-frequency communication systems. Tunable circuits embedded in communications systems will not only improve the performance of currently available facilities but also form a basis for radically new approaches that will impart self-organization (specifically, self-optimization) properties to mobile ultra-high-speed systems.

The BST permittivity can be changed by more than three times by applying a constant voltage at a current of <1 nA. The effect is fundamental for designing electronically controlled devices, such as filters, phase shifters, voltage controlled generators, and delay lines [1–3]. However, only laboratory prototypes of these devices have been created to date because of the unmatured technology of fabrication thereof and, as a consequence, the lack of reliable data for the ferroelectric state in (Ba, Sr)TiO_3/MgO structures with nanodimensional films.

The change in the ferroelectric state is associated with high internal stresses present in thin films. They are due to a substrate–film lattice mismatch, considerable difference between the linear thermal expansion coefficients of the film and substrate, and spontaneous polarization attendant on the paraelectric–ferroelectric transition after the heterostructure is formed. As a result, the film experiences mechanical-stress-induced structural modifications, which, in turn, change the characteristics of the phase transition and internal polarization states [4–9]. Naturally, the dependence of the permittivity on the external magnetic field takes another form, especially in the case of nanodimensional ferroelectric films.

In this work, we investigate the structural and insulating characteristics of nanodimensional epitaxial BST films.

EXPEREIMENT AND DISCUSSION OF RESULTS

$Ba_{0.8}Sr_{0.2}TiO_3$ films were applied on single-crystalline MgO(001) substrates by the high-frequency sputtering of stoichiometric targets of the same composition at an elevated oxygen pressure [9–11]. This technique differs from more conventional ones mainly in that a high-current rf discharge is used to provide the layer-by-layer growth of the films.

An rf power density of 70 W/cm^2 applied to the electrodes and a high oxygen pressure (0.5 Torr) made it possible to generate microparticles of the initial oxide in the plasma, which served as the vapor phase for the growing film. The substrate temperature during deposition was kept at 650°C. The film growth was monitored using optical spectroscopy data for the spatial distribution of sputtered components. That the film grew by the layer-by-layer mechanism and had an atomically smooth surface was confirmed by the

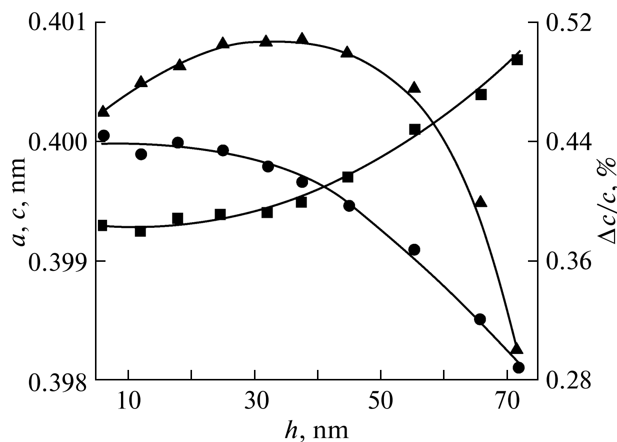

Fig. 1. Unit cell parameters (■) c and (●) a and (▲) strain nonuniformity $\Delta c/c$ vs. film thickness h.

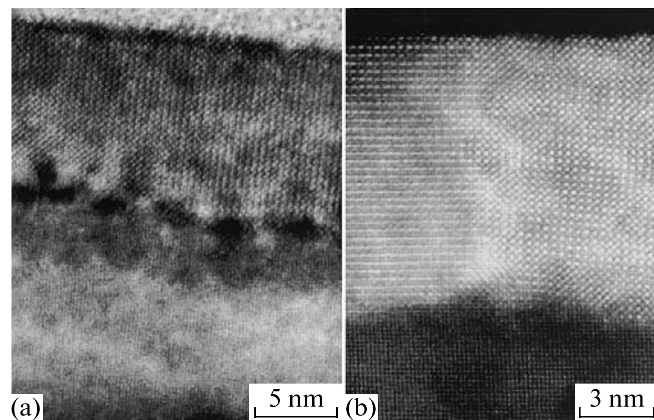

Fig. 2. Micrographs taken of the BST/MgO heterostructure: (a) 12-nm-thick film (low magnification) and (b) atomic-resolution STEM image of this film revealing a local misorientation of blocks around the vertical axis.

methods of electron microscopy and atomic-force microscopy.

The surface roughness averaged over the film was ≈0.4 nm. The thickness L of the films more than 100 nm thick was determined with an MII-4 microinterferometer; otherwise ($L < 100$ nm), it was measured from the sputtering time (with regard to the fact that the deposition rate of thicker films was 10.5 nm/min) and also using the micrographs of their cross sections.

The structural perfection of the films, unit cell parameters in the directions normal and parallel to the substrate plane, and orientation relationships between the substrate and film at room temperature were determined by the X-ray diffraction technique using a DRON-4 diffractometer equipped with a GP-14 goniometer head for texture examination (CuK_α radiation, Θ–2Θ geometry, recording of symmetric and asymmetric Bragg reflections). X-ray diffraction analysis showed that the intensity of diffraction maxima from the films more than 5 nm thick suffice to reliably determine both the unit cell parameters and film–substrate orientation relationships.

The parameter c of the unit cell in the direction normal to the film was found using a (00l) reflection, cell parameters a in the substrate film were found from allowable (h0l) reflections, and parameter b was determined using an equivalent set of reflections (with permutation of indices h and k). Cell parameters a and b were calculated in the orthorhombic approximation. In all the films, the axes of the film and substrate ran parallel to each other at the interface; that is, $[100]_{BST}||[100]_{MgO}$, $[010]_{BST}||[010]_{MgO}$, and $[001]_{BST}||[001]_{MgO}$. This points to film–substrate tight coupling, because of which parameters a and b are equal to each other and the respective axes make a right angle. The mosaicity (vertical misorientation) of the films was ≈0.6°. From the half-widths of asymmetric reflections from the films recorded when the counter and sample were fixed and the entire structure rotated about the normal to the substrate plane (the φ method), it followed that the azimuthal misorientation was less than 0.5°.

The X-ray diffraction analysis of the films carried out at room temperature revealed singularities in the dependences of the lattice parameters on the film thickness (Fig. 1). At thicknesses less than 40 nm, lattice parameter a (in the substrate plane) is larger than lattice parameter c (in the direction normal to the plane); that is, the films possess tensile stresses in the substrate plane and $c/a < 1$. If the films are more than 40 nm thick, the lattice parameter along the normal to the substrate grows and becomes larger than in-plane parameter a, which decreases as the film gets thicker ($c/a > 1$). In this thickness range, tensile stresses in the films change sign, becoming compressive stresses. Thus, there exists a critical thickness of the film (≈40 nm) below which the films contain tensile stresses in the plane of the substrate; above this value, they turn into compressive stresses.

Figure 1 also shows the thickness dependence of strain nonuniformity $\Delta c/c$ determined from the broadening of (001) and (002) reflections. It is seen that a strain gradient is present across the depth of the film. This strain gradient is due to the nonuniform distribution of defects (vacancies, dislocations, etc.) and may strongly influence both the insulating properties of the films and the position of the permittivity maximum.

The structure of the nanodimensional film–substrate interface was examined under Tecnai G230ST and FEI Titan 80–300 electron microscopes equipped with a high-angle annular dark-field detector and operating in the transmission–scanning mode (HAADF STEM) at an accelerating voltage of 300 kV. The micrographs of the barium strontium titanate films and BST–MgO interface were taken from cross sections and special samples prepared by mechanical

grinding and ion milling using a Gatan PIPS setup (model 691) with an ion energy of 4.5–5.0 keV.

Figure 2a shows a micrograph taken of the 12-nm-thick film (at a low magnification) on the MgO substrate. The surface of the film is seen to be smoother than the film–substrate interface, on which a periodic contrast typical of all the films whatever their thickness, is present. Main reasons for this contrast are misfit dislocations arising because of a film–substrate lattice misfit; misorientation of mosaic blocks in the film, which was found by the X-ray diffraction method; and a polishing-induced surface microrelief on the MgO substrate.

The atomic-level examination of the structure using high-resolution electron microscopy revealed the azimuthal misorientation of some parts of the film by 0.6°. Figure 2b demonstrates the atomic-resolution STEM image of the boundary between two misoriented parts. The primary reason for this misorientation seems to be the poor quality of polishing of the MgO substrate, which changes the substrate relief, as shown in Fig. 2b.

Dislocations were visualized with the method of indirect lattice resolution using moiré patterns [12]. When two crystal lattices are superimposed, a moiré pattern arises due to a lattice mismatch (parallel moiré pattern) or different misorientations (rotation moiré pattern).

Figure 3a shows the moiré pattern obtained by superposing the BST and MgO lattices. The period D of the moiré pattern calculated by the formula $D = d_1d_2/(d_1 - d_2)$, where d_1 and d_2 are in the interplanar spacings of the superimposed lattices, equals 3.8 nm. On the high-resolution filtered image of the crystal lattice (Fig. 3b), a dislocation with a [100] Burgers vector is seen in the film against the moiré pattern background.

Thus, by analyzing the moiré patterns and filtering high-resolution images, we found that the moiré pattern is parallel, i.e., is due to a MgO–BST lattice mismatch, and allows dislocation visualization.

High-resolution electron microscopy (HREM) makes it possible to directly visualize the atomic structure of test objects. To visualize lattice distortions at the film–substrate (BST–MgO) interface, we applied programs based on the geometrical phase analysis [12].

The images shown in Fig. 4 reflect the stages of this analysis as applied to the structure of the 6-nm-thick film. The first stage (Fig. 4a) is the formation of a high-resolution bright-field image of the interface and construction of its corresponding Fourier transform (Fig. 4b) with the Digital Micrograph routine program package. For varying lattice periods, the Fourier coefficients are a function of coordinates. In the reciprocal space, this function represents the intensity distribution around a corresponding reflection and can be derived by the inverse Fourier transformation of the domain around this reflection. In this way, one can

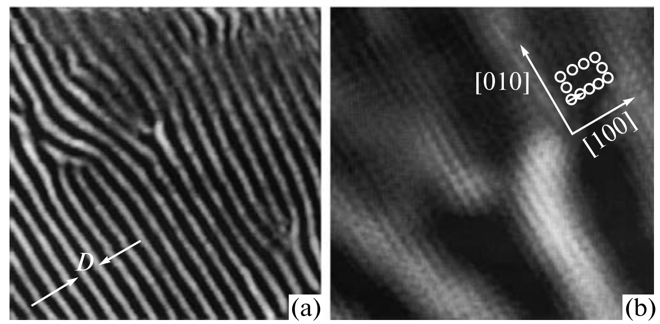

Fig. 3. (a) Parallel moiré pattern arising upon the superposition of the BST and MgO lattices and (b) high-resolution filtered image of the lattice against the background of the moiré pattern.

obtain a field of phase shifts, which can be viewed as a displacement field for a given set of planes or as a local variation of the lattice parameter. Figure 4c maps the interplanar spacing distribution for the (020) reflection. The periodic contrast along the interface in the form of black-and-white rosettes is due to alternating compression (dark) and extension (bright) fields. Such a distortion pattern is associated with strains near dislocation cores.

Since the intensity at each point is related to the local value d of the interplanar spacing for {010} planes, one can argue that d is constant in the substrate. As for the 6-nm-thick film, the value of d in it is nearly the same as d in the substrate. This means that the film is extended at the interface.

Having imposed the image obtained with the program for the geometrical phase analysis on the image of the set of planes {010} (Fig. 4d), one can see that the periodic black-and-white contrast arises at the sites of extraplane emergence or BST lattice distortion.

Figure 5 shows the images of the interface for the films 6 and 12 nm thick on which the characteristic contrast near dislocation cores is seen. For the latter film, the value of d decreases compared with that for the former; however, the film remains tetragonally distorted at the interface. For the 12-nm-thick film, the period of the characteristic black-and-white contrast appearing at the interface, 5–6 nm, is almost twice as small as that for the 6-nm-thick one. This indicates that stresses in the films relax as they get thicker owing to the emergence of extraplanes.

Thus, the strain relaxation governing the mechanical unloading of the nanodimensional BST film is due primarily to the generation of misfit dislocation. Physically, the process can be represented as the slippage of the film over the substrate without detaching. Gaining insight into these effects is of extreme importance when an attempt is made to grow BST films with a microstructure providing maximal permittivity. How-

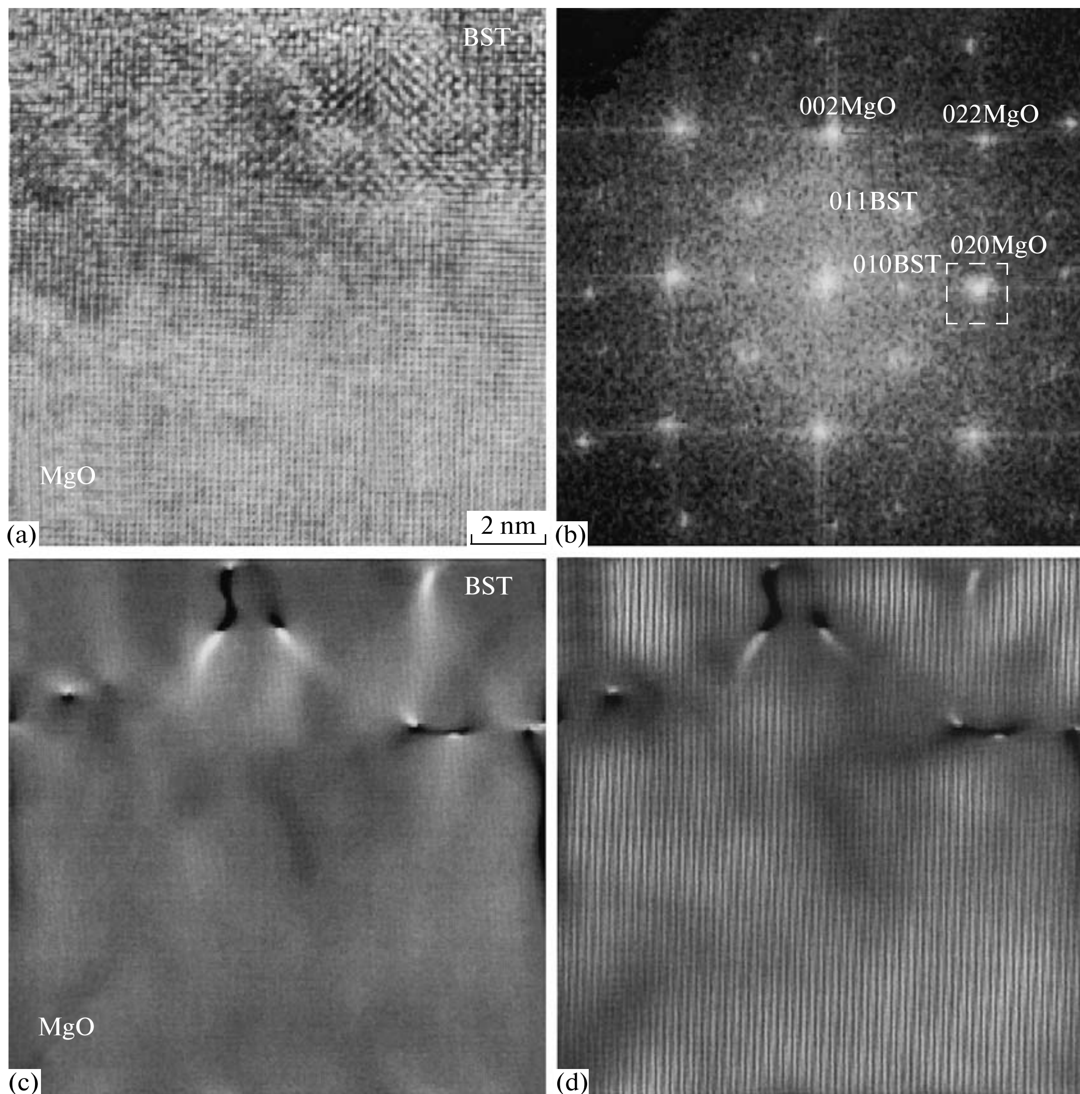

Fig. 4. Analysis of the HREM images of lattice distortions: (a) atomic-resolution image of the 6-nm-thick film, (b) Fourier transform of the image depicted in panel (a), (c) distribution map of interplanar spacings that was obtained by the geometrical phase method, and (d) superposition of panel (c) on the image of the set of {010} planes.

ever, dislocations make the polarization distribution over the depth of the film nonuniform.

It is natural to expect that stresses present in the film influence its insulating properties. To check this supposition, we applied planar interdigitated electrodes with 440 fingers on the film by lift-off lithography (inset in Fig. 6). The length and width of the fingers and the finger spacing were 130.0, 1.3, and 1.1 μm, respectively.

The capacitance, conductivity, and leakage current of the plane capacitors were measured by a Keithley 4200SCS semiconductor characterization system at a frequency of 1 MHz using a Micro Tec PM-5 probe station. The variation of the normalized capacitance with the applied voltage at a frequency of 0.05 Hz is shown in Fig. 6 for the films with various thicknesses. It is seen that the dielectric reconstruction of the film becomes more pronounced with an increase in its thickness. Taking into consideration that the dislocation spacing in the 6-nm-thick film is twice as large as that in the 12-nm-thick one, we can relate reconstruction coefficient K,

$$K = \varepsilon(E_{\text{bias}} = 0)/\varepsilon(E_{\text{bias}} \neq 0),$$

where E_{bias} is the control electric field to the relaxation of the internal strain field. In fact, the dislocation spacing in the 6-nm-thick film is 11–14 nm versus 5–6 nm in the film 12 nm thick. Accordingly, the controllability coefficient grows from 1.03 to 1.20. Therefore, one can suppose that much of the stresses relaxed in the 32-nm-thick film, as a result of which the controllability coefficient increased to 2.3.

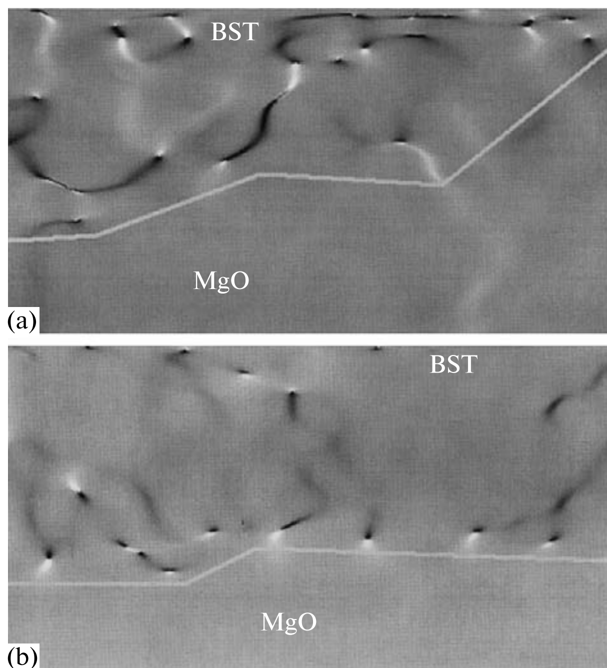

Fig. 5. Distribution map of interplanar spacings that was obtained by the geometrical phase method for the films (a) 6 and (b) 12 nm thick.

CONCLUSIONS

$Ba_{0.8}Sr_{0.2}TiO_3$ ferroelectric heteroepitaxial films grown on MgO(001) substrates by the layer-by-layer mechanism are single-crystalline. However, they contain misfit dislocations resulting from stress relaxation and have a mosaic (block) structure with a small misorientation (0.5°) due primarily to the substrate surface relief.

The moiré pattern arising upon the superposition of the BST and MgO lattices reveals dislocations with ⟨100⟩ and 1/2⟨110⟩ Burgers vectors, which outline the boundaries of the blocks.

The digital processing of HREM micrographs taken of the cross section of the BST/MgO heterostructure made it possible to visualize lattice distortions at the interface and show that stresses in the films relax through the formation of misfit dislocations at the interface.

It is shown that the stress relaxation due to the formation of misfit dislocations is necessary for the coefficient of capacitance reconstruction under the action of an external field be high.

ACKNOWLEDGMENTS

The authors thank Prof. Ute Kaiser, University of Ulm, for enabling investigations in the laboratory she heads.

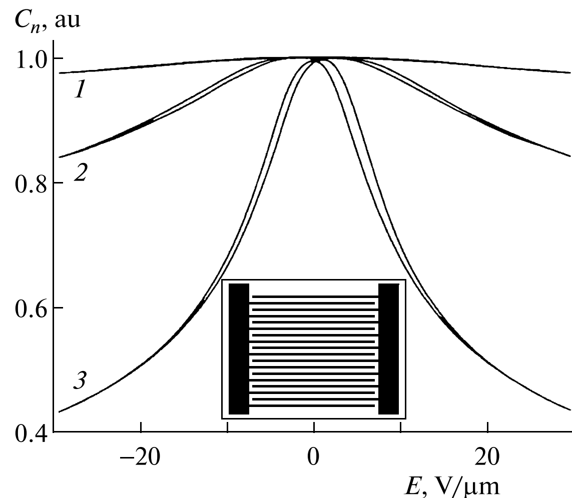

Fig. 6. Dielectric nonlinearity of the nanodimensional films (*1*) 6, (*2*) 12, and (*3*) 32 nm thick.

This work was supported by the Russian Foundation for Basic Research, grant nos. 08-02-13511-ofi_ts and 09-02-00254-a.

REFERENCES

1. A. Kozyrev, V. Osadchy, A. Pavlov, and L. Sengupta, IEEE MTT-S Int. Microwave Symp. Dig. **3**, 1355 (2000).
2. H. C. Ryu, S. E. Moon, Y. T. Kim, M. H. Kwak, S. J. Lee, K. Y. Kang, and S. O. Park, J. Korean Phys. Soc. **48**, 1637 (2006).
3. B. Acikel, T. R. Taylor, P. J. Hansen, J. S. Speck, and and R. A. York, IEEE Microwave Wireless Comp. Lett. **12**, 237 (2002).
4. G. A. Smolensky, *Ferroelectrics and Related Materials* (Gordon and Breach, New York, 1985), p. 512.
5. J. A. Bellotti, E. K. Akdogan, A. Safari, W. Chang, and S. W. Kirchoefer, Integr. Ferroelectr. **49**, 113 (2002).
6. W. J. Kim, H. D. Wu, W. Chang, S. B. Qadri, J. M. Pond, S. W. Kirchoefer, D. B. Chrisey, and J. S. Horwitz, J. Appl. Phys. **88**, 5448 (2000).
7. W. Chang, S. W. Kirchoefer, J. M. Pond, J. A. Bellotti, S. B. Qadri, J. H. Haeni, and D. G. Schlom, J. Appl. Phys. **96**, 6629 (2004).
8. Yu. I. Golovko, V. M. Mukhortov, and A. A. Mamatov, Vestn. Yuzhn. Nauchn. Tsentr. RAN **4** (2), 11 (2008).
9. V. M. Mukhortov, A. A. Mamatov, P. A. Zelenchuk, Yu. I. Golovko, S. V. Biryukov, and S. I. Masychev, Nanotekhnika **3** (11), 59 (2007).
10. V. M. Mukhortov, Yu. I. Golovko, V. V. Kolesnikov, V. V. Biryukov, A. A. Mamatov, and Yu. I. Yuzyuk, Zh. Tekh. Fiz. **77** (10), 103 (2007) [Tech. Phys. **52**, 1345 (2007)].
11. V. V. Mukhortov and Yu. I. Yuzyuk, *Heterostructures Based on Nanometric Ferroelectric Films: Production, Properties and Applications* (YuNTs RAN, Rostov-on-Don, 2008), p. 224.
12. A. K. Gutakovskii, A. L. Chuvilin, and Song Se Ahn, Izv. Ross. Akad. Nauk, Ser. Fiz. **71**, 1464 (2007).